JOURNAL OF MATERIALS SCIENCE 25 (1990) 2476–2480

The effect of composition, substrate temperature and annealing on the paramagnetic centres in SiO_x/SnO co-evaporated thin films

G. A. KHAN, C. A. HOGARTH, K. A. LOTT*
*Department of Physics and *Department of Chemistry, Brunel University, Uxbridge, Middlesex, UK*

The effects of composition and substrate temperature during evaporation and annealing, on the electron spin resonance spectra of co-evaporated SiO_x/SnO (300 nm) thin films have been investigated. The spin density is observed to decrease with increasing SnO content. This effect is attributed to the saturation of some of the paramagnetic defects such as dangling bonds and other structural defects like E_1' centres. The decrease in spin density in the composite thin films of SiO_x/SnO of constant thickness and composition with annealing and with increase in the substrate temperature during evaporation, is related to the conversion of some of the paramagnetic E_1' centres to E_1'' (probable non-paramagnetic precursor of E_1') centres as well as to the saturation of some of the dangling bonds.

1. Introduction

It has been agreed that in the forbidden gap of amorphous semiconductors there exist localized charged states which might be attributed to dangling bonds, impurities or other defects in the structure of disordered solids. Various optical and electronic studies of chalcogenide glasses have been interpreted in terms of such localized states. To investigate the electronic properties of amorphous semiconductors, the electron spin resonance (ESR) techniques are especially studied for macroscopic identification of electronic defect states [1–4]. The most important interactions in dilute electronic spin systems, namely the spin orbit and hyperfine coupling, are sensitive to the chemical nature of the atoms involved, so that it is possible to distinguish between the same type of defect in different chemical environments. The characteristics of the ESR technique are important in semiconducting alloy systems such as hydrogenated amorphous silicon-germanium (a-SiGe:H) alloy. ESR spectra of undoped a-SiGe:H have been used to distinguish between dangling bond defects localized on silicon and germanium [5, 6]. Street and Mott [7] while studying As_2Se_3, measured the concentration of dangling bonds in the range 10^{18} to 10^{19} cm^{-3}. They suggested that the dangling bonds may be occupied by zero, one or two electrons and labelled these states D^+, D^0 and D^-, respectively. Kastner *et al.* [8] equivalently used C^+ and C^- for these defect centres, where C stands for a chalcogen atom. Bishop *et al.* [9] proposed that in chalcogenide glasses, the optically induced ESR and the absorption were due to localized paramagnetic states in the forbidden gap. They showed that these centres are the holes localized on chalcogens and are not directly associated with the impurities.

Vacuum-evaporated thin films of SiO vary strongly in composition, depending upon the deposition rate and the oxygen partial pressure. Many reports have been published on optical [10–12] and electrical [13, 14] properties. However, there are some ambiguities concerning the defects in SiO and the existence of the chemical compound in the solid state [15]. Timson and Hogarth [16] measured spin densities between 10^{18} to 10^{20} cm^{-3}, which correspond to the samples with varying oxygen contents covering the range of composition from SiO_2 to SiO. They supposed that the ESR signals originate from unpaired electrons on dangling bonds. Such silicon atoms with unsaturated bonds can be regarded as donor centres responsible for the Poole–Frenkel effect. Feigl and Anderson [17] reported that ESR in SiO was due to an electron in an sp^3 nonbonding directed orbital in an unrelaxed silicon facing an oxygen vacancy. However, Weeks and Nelson [18] considered an electron trapped at an unrelaxed oxygen vacancy to be responsible for the ESR signal. They proposed three types of such structural defects as shown below.

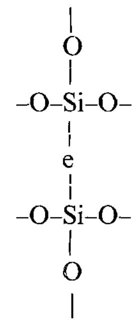

$$\begin{array}{c} | \\ \text{O} \\ | \\ \text{-O-Si-O-} \\ | \\ \text{e} \\ | \\ \text{-O-Si-O-} \\ | \\ \text{O} \\ | \end{array} \qquad (1)$$

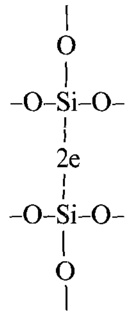

$$\begin{array}{c} | \\ \text{O} \\ | \\ \text{-O-Si-O-} \\ | \\ \text{2e} \\ | \\ \text{-O-Si-O-} \\ | \\ \text{O} \\ | \end{array} \qquad (2)$$

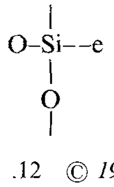

$$\begin{array}{c} \text{O} \\ | \\ \text{O-Si--e} \\ | \\ \text{O} \\ | \end{array} \qquad (3)$$

0022-2461/90 $03.00 + .12 © *1990 Chapman and Hall Ltd.*

Defects 1, 2 and 3 are referred to as E_1', E_1'' and E_2' centres, respectively. E_1' is the electron occupation defect usually resulting in a net spin moment, E_1'' represents the two electrons trapped at the defect which is a non-paramagnetic precursor of E_1', and E_2' is the paramagnetic centre giving an ESR signal at a different g-value compared to that for E_1' [11, 18–20]. Paez *et al.* [21] suggested that amorphous thin films of silicon oxide deposited by the evaporation of silicon monoxide powder showed an unresolved ESR signal with a g value between 2.006 and 2.014. They observed spin densities of the order of $10^{19}\,\mathrm{cm^{-3}}$, the values depending strongly on the preparation and annealing conditions. The authors suggested that unsaturated oxygen bonds were responsible for the ESR signal. Mizutani *et al.* [22] indicated two types of paramagnetic centres in SiO, which were associated with the broad and narrow signals. The authors assigned the broad signal at $g = 2.0025 \pm 0.0003$ to $\mathrm{SiO_{3/2}}\ (-\overset{|}{\underset{|}{\mathrm{Si}}}\uparrow)$, where the symbol in parenthesis indicates an unpaired electron spin. The narrow signal appeared at $g = 2.0025 \pm 0.0003$ after heating SiO powder in vacuum at a temperature between 1273 and 1473 K. On exposure to oxygen, the signal height decreased and the line was broadened as a result of dipolar interaction of oxygen molecules absorbed on to the surface with the ESR centres, indicating that the centres lie on or near the surface.

Timson and Hogarth [16] were the first to investigate the ESR in composite $\mathrm{SiO/B_2O_3}$ thin films. They observed a decrease in spin density with increase in $\mathrm{B_2O_3}$ content. Dubey *et al.* [23] confirmed these results. Arshak and Hogarth [24] considered the effect of composition and annealing on ESR in SiO/BaO and observed a decrease in ESR signal which was attributed to the saturation of some of the dangling bonds. Recently, Razzaq *et al.* [25] observed a decrease in the ESR signal with increasing $\mathrm{CeO_2}$ content in $\mathrm{SiO/CeO_2}$ composite thin films. They related this decrease in ESR signal to the loss associated with the distribution of diamagnetic $\mathrm{Ce^{4+}}$ ions in the film matrix and some local cross bonding between the $\mathrm{CeO_2}$ and SiO components of the thin films.

Therefore, the interpretation of ESR spectra of SiO_x is still a matter of debate. We have investigated the variation of paramagnetic centres in composite SiO_x/SnO thin films with the increase in the content of SnO. The dependence of ESR signal on substrate temperature during deposition and on annealing of samples of constant thickness and composition of mixed SiO_x/SnO oxide thin films is also studied.

2. Experimental procedure

The samples of co-evaporated SiO_x/SnO thin films of different compositions and constant thickness (300 nm) were deposited from analytical reagent grade materials on to a precleaned borosilicate 3 cm × 1 cm substrate fused on to two glass rods of 4 and 6 cm lengths, to fit the ESR spectrometer. The Speedivac Coating Unit model 19A/122 at a pressure of the order of 10^{-6} torr (1.33×10^{-4} Pa) was used for the co-evaporation of oxides following the technique which has already been established and described by Hogarth and Wright [16]. Silicon monoxide and tin monoxide were evaporated from tantalum and tungsten boats, respectively. The evaporation parameters such as composition and thickness of the films were monitored by means of a quartz crystal monitoring system which was calibrated for each material. The total thickness of co-evaporated oxide thin films was measured by multiple beam interferometry making use of Fizeau fringes of equal thickness. The ESR measurements were made at room temperature using a Varian E3-EPR spectrometer working at the X-band at the same modulation amplitude, time constant and magnetic field scan for each sample. The amplifier sensitivity was changed for some samples to give a measurable signal trace. The area under the curve of second integral of output ESR signal is directly proportional to the spin density. The value so derived is used in conjunction with the sample volume and the sensitivity of the instrument to calculate the value of spin density. The spectrometer was calibrated in absolute spins $\mathrm{cm^{-3}}$ using an aqueous copper sulphate solution of known spin concentration and contained in a pyrex cell. The measurements were made for the same magnetic field of 3400 G and at a microwave frequency of 9.3 GHz for all samples. In order to investigate the effect of substrate temperature during evaporation on the spin density of a given composition and thickness of SiO_x/SnO mixed oxide system, the temperature was varied from 293 to 593 K in steps. Finally, the samples of SiO_x/SnO of constant thickness and composition were annealed for 2 h at different temperatures to study the annealing effect on paramagnetic centres in SiO_x/SnO mixed amorphous thin films.

3. Results

SiO_x (300 nm) thin films showed a strong ESR signal, as can be seen in Fig. 1a. The value of g is very close to the free spin value. Fig. 1b shows the intensities of the ESR signals of composite SiO_x/SnO (300 nm) films with different SnO content. It is observed that the signal intensity goes on decreasing with increasing content of SnO in SiO_x/SnO thin films. The variation of spin density with the variation of SnO concentration in SiO_x/SnO co-evaporated thin films is shown in Fig. 2. The intensity of the ESR signal decreases very slowly with increasing substrate temperature (during evaporation) up to 493 K and afterwards it decreases at a higher rate as indicated in Fig. 3. The change in the spin density with the substrate temperature (during evaporation) is shown graphically in Fig. 4. Similarly, the annealing effect shows a slow decrease in ESR signal intensity up to 473 K, and beyond this temperature the signal intensity decreases noticeably as can be seen in Fig. 5. Fig. 6 shows a plot of calculated spin density against annealing temperature of 90% SiO_x/10% SnO (300 nm) thin films.

4. Discussion

The decrease in the spin density of composite SiO_x/SnO thin films with the increase in SnO content can be

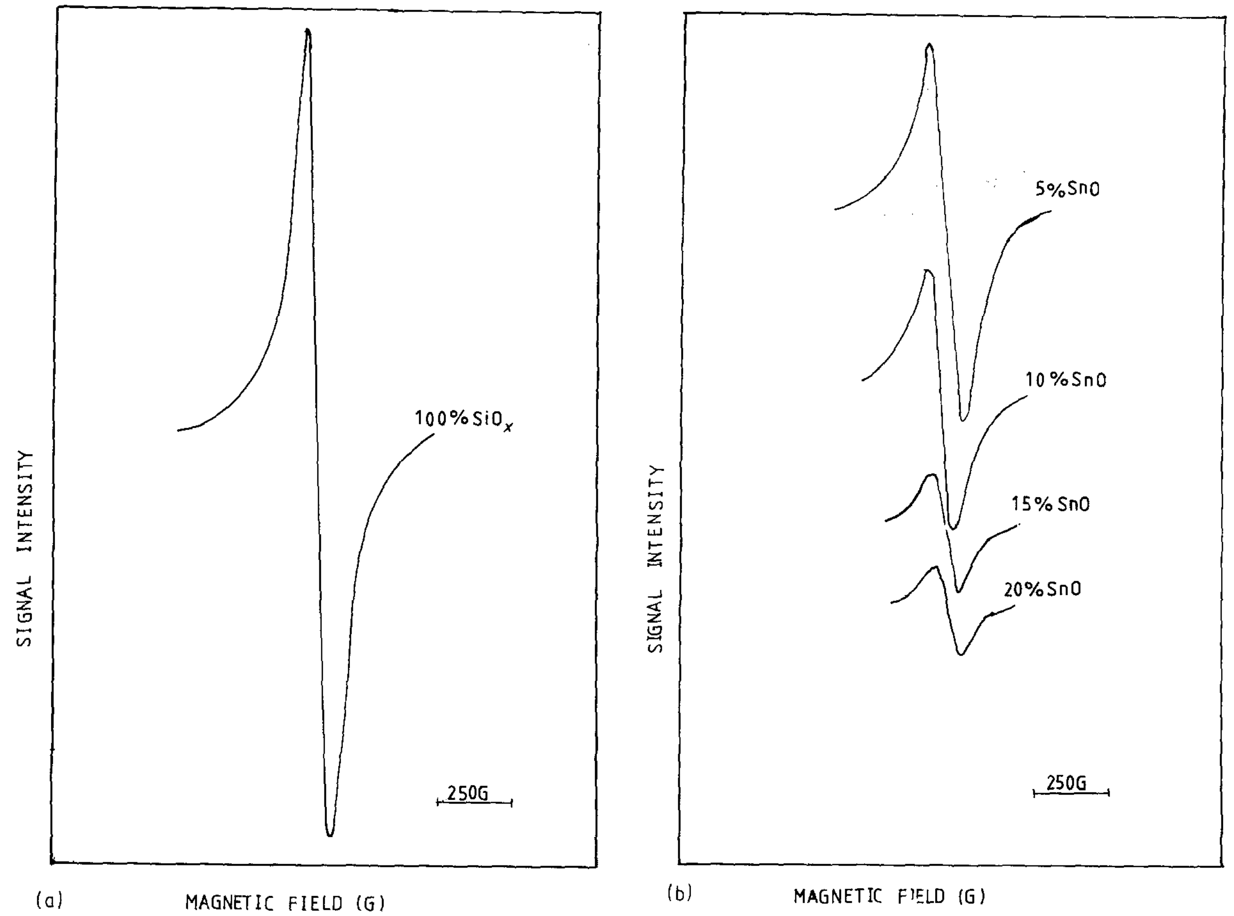

Figure 1 ESR spectra of (a) SiO_x (300 nm) thin film and (b) SiO_x/SnO (300 nm) thin films of different compositions, at 2×10^5 gain.

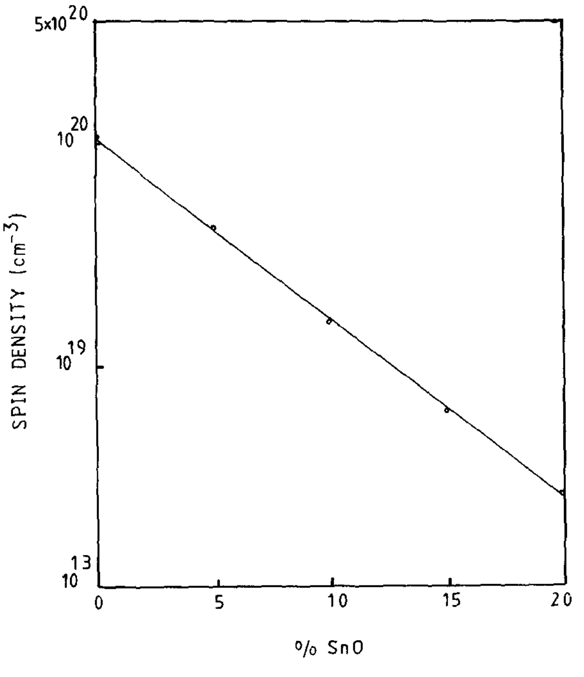

Figure 2 Spin density of SiO_x/SnO (300 nm) thin films as a function of SnO concentration.

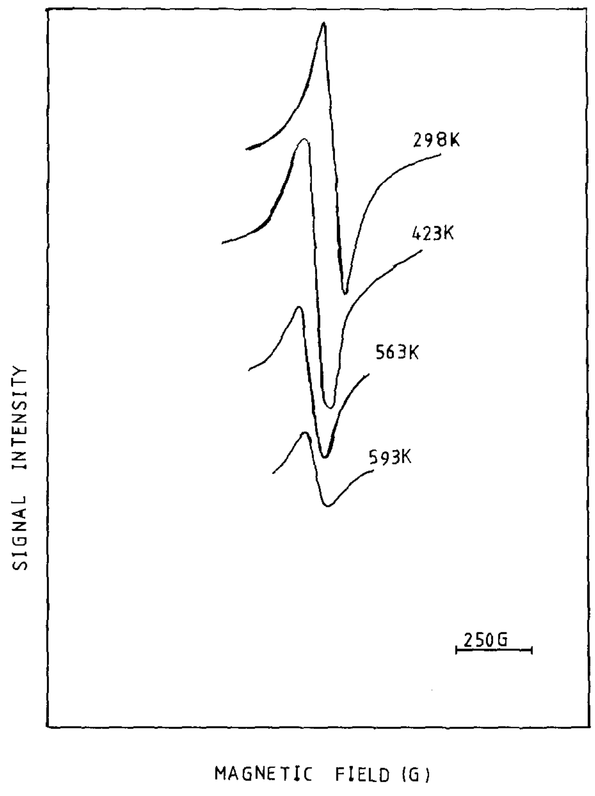

Figure 3 ESR spectra of 90% SiO_x/10% SnO (300 nm) thin films prepared at different substrate temperatures during evaporation (2×10^5 gain).

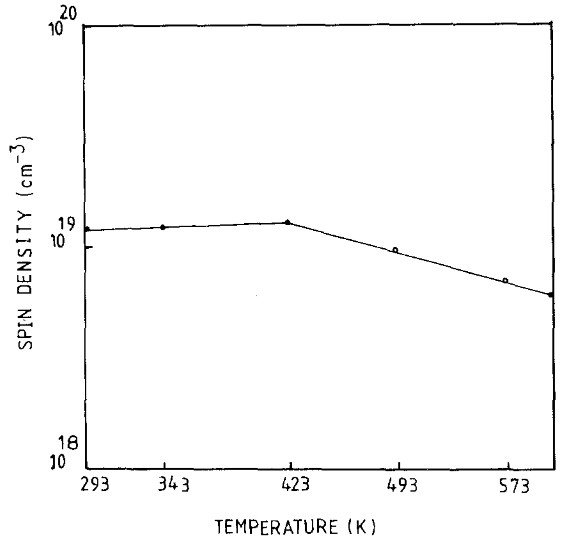

Figure 4 Spin density of 90% SiO_x/10% SnO (300 nm) thin films as a function of substrate temperature during evaporation.

interpreted in the following way. Vacuum-evaporated SiO_x thin films can be regarded as an extended chain compound which in combination with O_2 forms a stable, paramagnetic silicon hyperoxide structure in accordance with the reaction proposed by Schiller and Beister [26]. The simplified reaction can be written as

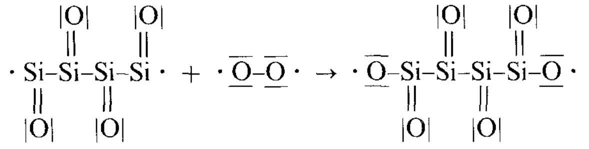

$$\cdot\underset{\underset{|O|}{\|}}{Si}-\overset{\overset{|O|}{\|}}{Si}-\underset{\underset{|O|}{\|}}{Si}-\overset{\overset{|O|}{\|}}{Si}\cdot + \cdot\overline{\underline{O}}-\overline{\underline{O}}\cdot \rightarrow \cdot\overline{\underline{O}}-\underset{\underset{|O|}{\|}}{Si}-\overset{\overset{|O|}{\|}}{Si}-\underset{\underset{|O|}{\|}}{Si}-\overset{\overset{|O|}{\|}}{Si}-\overline{\underline{O}}\cdot$$

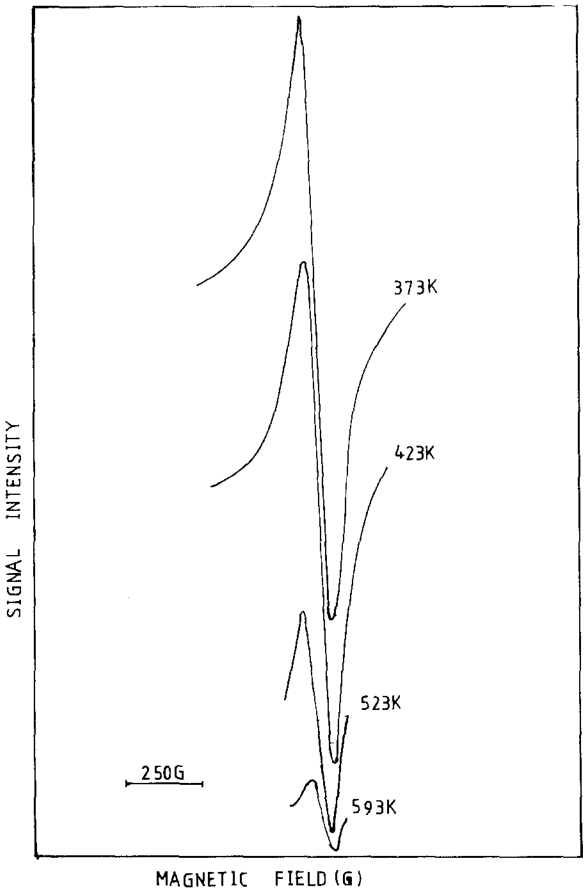

Figure 5 ESR spectra of 90% SiO_x/10% SnO (300 nm) thin films after annealing at different temperatures (3.2 × 10^5 gain).

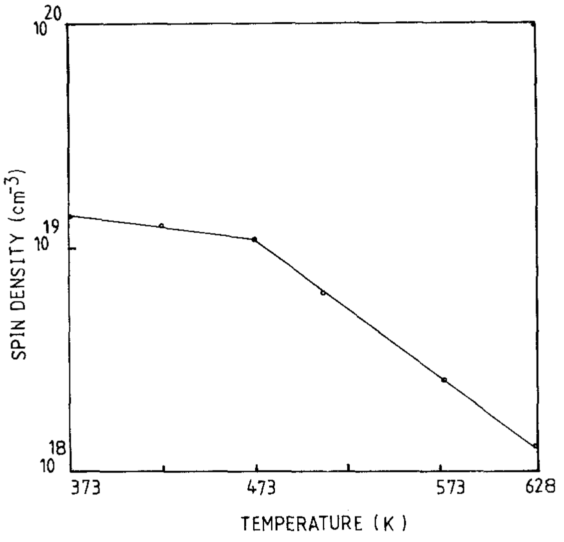

Figure 6 Spin density of 90% SiO_x/10% SnO (300 nm) thin films as a function of annealing temperature.

where bars around the oxygen denote free electron pairs. Thus two paramagnetic radical structures may exist in SiO_x as

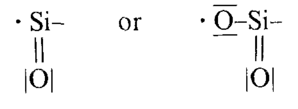

$$\cdot\underset{\underset{|O|}{\|}}{Si}- \quad \text{or} \quad \cdot\overline{\underline{O}}-\underset{\underset{|O|}{\|}}{Si}-$$

The structure and composition of evaporated tin oxide films depends on the conditions during deposition and following heat treatment [27–30]. Neumann *et al.* [31] suggested that the relaxed short-range order configuration of amorphous thin films of SnO_x correlates well with the intermediate crystalline tin oxide, Sn_2O_3. We propose that the existence of such an intermediate oxide phase (Sn_2O_3) in our films is most probably due to the reaction of the type which can be written as

$$Sn^{2+} \rightarrow Sn^{3+} + e^-$$

$$2Sn^{3+} + 3O^{2-} \rightarrow Sn_2O_3$$

The electron set free during the above reaction may reside on one of the dangling bonds of oxygen or silicon as the case may be, to convert the dangling bond to a charged state which reduces the paramagnetic character of the dangling bond. Similarly if there exist some other structural defects such as E_1' in our samples, then the electron released during the formation of Sn_2O_3 may also be captured by such a centre to convert it into E_1'' which is non-paramagnetic. This phenomenon will also reduce the resultant spin density.

A very important process during the film formation under reactive gases is chemisorption. One of the factors that has a strong bearing on the sorption is the substrate temperature during film formation [26]. While making measurements of the ESR in tin oxide Chang [32] proposed that the chemisorbed oxygen in tin oxide consists of O^{1-}, O_2^{1-} and O^{2-}, where O^1 and O_2^{1-} are paramagnetic and O^{2-} with its filled orbit is non-paramagnetic (not detectable by ESR technique). The author observed an interconversion in ESR signal related to O^{1-} and O_2^{1-} with the variation of temperature. He observed a decrease in the ESR in tin oxide as the temperature of the sample was increased beyond 473 K. The decrease in the ESR signal in tin oxide films beyond 473 K (the inversion temperature) was attributed to the formation of O^{2-} species. The annealing and the substrate temperature effect during the co-evaporation of SiO_x/SnO thin films of a given composition and thickness in our case can be explained in a similar way. A noticeable decrease in the spin density starts in the temperature range 420 K to 473 K in the present case which is in good agreement with the results shown by Chang [32] in tin oxide. So the decrease in ESR signal in given composite SiO_x/SnO thin films with the annealing and with the substrate temperature during evaporation is attributed to the similar behaviour of SnO in composite SiO_x/SnO films in which the conversion of chemisorbed oxygen species O^{1-} or O_2^{1-} to O^{2-} may occur.

5. Conclusion

The electron spin resonance phenomena in SiO_x/SnO may be related to the dangling bonds of silicon and to the existence of E_1' centres. The decrease in spin density with the increasing content of SnO in SiO_x/SnO composite films is attributed to the conversion of some of the E_1' centres to non-paramagnetic E_1'' centres. The reduction in the density of paramagnetic centres in SiO_x/SnO with annealing and higher substrate temperature during deposition is related to the conversion of O^{1-} to O^{2-} in SnO.

References

1. M. STUTZMANN, O. K. BIEGELSEM and R. A. STREET, *Phys. Rev. B.* **35** (1987) 5666.
2. M. STUTZMANN, J. STUKE and H. DERSEH, *Phys. Status Solidi (b)* **115** (1983) 141.
3. N. F. MOTT, "Amorphous and Liquid Semiconductors" (North Holland, Amsterdam, 1970).
4. H. DERSEH, J. STUKE and J. BEICHER, *Phys. Status Solidi (b)* **105** (1981) 265.
5. M. KUMEDA, Y. JINNO and T. SHIMIZU, *ibid.* **81** (1977) K71.
6. A. MORIMOTO, T. MIURA, M. KUMEDA and T. SHIMIZU, *Jpn J. Appl. Phys.* **20** (1981) L833.
7. R. A. STREET and N. F. MOTT, *Phys. Rev. Lett.* **35** (1975) 1293.
8. M. KASTNER, D. ALDER and H. FRITZSCHE, *ibid.* **37** (1976) 1504.
9. S. G. BISHOP, U. STROM and P. C. TAYLOR, *ibid.* **34** (1975) 1346.
10. A. L. SHABALOV and M. S. FELDMAN, *Thin Solid Films* **151** (1987) 317.
11. C. M. NELSON and R. A. WEEKS, *J. Amer. Ceram. Soc.* **43** (1960) 396.
12. D. REDFIELD, *Phys. Rev.* **130** (1963) 916.
13. S. MANHART, *J. Non-Cryst. Solids* **11** (1973) 293.
14. M. S. FROST and A. K. JONSCHER, *Thin Solid Films* **29** (1975) 7.
15. G. SIDDALL, *Vacuum* **9** (1960) 274.
16. P. A. TIMSON and C. A. HOGARTH, *Thin Solid Films* **10** (1972) 321.
17. F. J. FEIGL and J. H. ANDERSON, *J. Phys. Chem. Solids* **31** (1970) 575.
18. R. A. WEEKS and C. M. NELSON, *J. Amer. Ceram. Soc.* **43** (1960) 399.
19. K. L. YIP and W. B. FOWLER, *Phys. Rev. B* **11** (1975) 2327.
20. R. A. WEEKS, *J. Appl. Phys.* **27** (1956) 1376.
21. R. PAEZ, L. C. HERNANDEZ, J. I. JARAMILLO, P. PRIETO, J. RODRIGUEZ and G. FRITSH, *J. Mag. Reson.* **29** (1978) 251.
22. T. MIZUTANI, O. OZAWA, T. WADA and T. ARIZUMI, *Jpn J. Appl. Phys.* **9** (1970) 446.
23. G. C. DUBEY, K. SAHU and T. R. REDDY, *Thin Solid Films* **61** (1979) L17.
24. K. I. ARSHAK and C. A. HOGARTH, *ibid.* **137** (1986) 281.
25. A. RAZZAQ, C. A. HOGARTH and K. A. K. LOTT, *Phys. Status Solidi* (*b*) **141** (1987) K61.
26. S. SCHILLER and G. BEISTER, *Surf. Coat. Tech.* **33** (1987) 367.
27. R. BANERJEE and D. DAS, *Thin Solid Films* **149** (1987) 291.
28. D. DAS and R. BANERJEE, *ibid.* **147** (1987) 321.
29. N. S. CHOUDHURY, R. P. GOEHNER, N. LEWIS and R. W. GREENE, *ibid.* **122** (1984) 231.
30. G. BEENSH-MARCHWICKA, L. KROL-STEPNIEWSKA and A. MISIUK, *ibid.* **113** (1984) 215.
31. H. G. NEUMANN, P. ZEGGEL and K. MELZER, *J. Non. Cryst. Solids* **108** (1989) 129.
32. S. C. CHANG, *J. Vac. Sci. Technol.* **17** (1980) 366.

Received 9 August
and accepted 12 September 1989